

Local Density Enhancement in Supercritical Carbon Dioxide Studied by Raman Spectroscopy

M. Isabel Cabaço,^{*,†} S. Longelin,[‡] Y. Danten,[‡] and M. Besnard[‡]

Centro de Física Atómica da UL, Av. Prof. Gama Pinto 2, 1694-003 Lisboa Codex and Departamento de Física, Instituto Superior Técnico, UTL, Av. Rovisco Pais 1049-001 Lisboa, Portugal, and Institut des Sciences Moléculaires, CNRS (UMR 5255), Université Bordeaux 1, 351 Cours de la Libération 33405 Talence Cedex, France

Received: July 19, 2007

The polarized I_{VV} and depolarized I_{VH} Raman profiles of the Fermi dyad (1285 cm^{-1} and 1388 cm^{-1}) of supercritical (SC) CO_2 have been measured along the isotherms 307, 309, 313, and 323 K in the reduced density range $0.04 < \rho^* = \rho/\rho_C < 2.04$ (ρ_C is the critical density). A band shape analysis of the dyad component shows that each one can be decomposed in two well-defined Lorentzian profiles in all of the temperature and density ranges investigated. These profiles have been assigned with the transitions of CO_2 probing two kinds of environments. In each dyad peak, the Lorentzian profiles centered at higher frequency is associated with CO_2 interacting through usual Van der Waals interactions with its nearest neighbors. The Lorentzian profiles centered at lower frequency in each dyad peak have been related to the transition of CO_2 involved in a transient $(\text{CO}_2)_2$ dimer. The evolution with the density of the band center positions and bandwidths of the Lorentzian profiles shaping the lower and upper dyad components exhibits a nonlinear behavior along the near critical isotherm (307 K) for ρ^* ranging from 0.4 to 1.7. This behavior, although less pronounced, is still detected at higher temperatures. The deviation from linearity was interpreted as being due to an enhancement of the density that leads to a reduced local density excess $\Delta\rho^* = \rho_{\text{loc}}^* - \rho_{\text{bulk}}^*$. Even if the spectroscopic observables involved probe the interactions in SC CO_2 differently, we emphasize that the scaled spectral features are straightforwardly related to the Local Density Enhancement (LDE) phenomenon taking place in SC fluids (SCF). We show that the LDE effect can also be put in evidence from the band shape analysis of the weak satellite band situated at 1370 cm^{-1} associated with the upper Fermi dyad transition of the $^{13}\text{C}^{16}\text{O}_2$ molecule (1% isotopic natural abundance). The asymmetric shape of the evolution with density of the $\Delta\rho^*$ found from our spectroscopic observables shows some similitude with that obtained in a recent MD simulation [Skarmoutsos, I.; Samios, J. J. *Chem. Phys.* 2007, 126, 44503.] and the possible inter-connection and difference with these calculations are discussed.

1. Introduction

One of the peculiarities of SCF is that it behaves as a hyper-compressible media in the vicinity of its critical point. As a consequence, small changes in pressure yield large changes in density. From the microscopic standpoint, SCF appears as inhomogeneous media with high and low-density regions extending over the length of the order of the correlation length, which characterizes the spatial range over which density fluctuations are correlated. Upon increasing the pressure at constant temperature along a near critical isotherm, the local density is enhanced compared to the bulk density of the corresponding homogeneous fluid.^{1–5} Theoretical and experimental studies agree on the fact that the typical behavior of the evolution of the local versus bulk density presents a three-regime behavior with a kind of plateau in a reduced density domain $\rho^* = \rho/\rho_C$ ranging roughly from 0.4 to 1.5. It is mostly in this density domain that the maximum relative local density enhancement (LDE) will occur at approximately $\rho^* = 0.6$ to 1.0. As a practical rule, LDEs are mostly observed in the reduced temperature range $T^* = T/T_C \leq 1.06$, whereas they become reduced and almost vanish at $T^* \geq 1.1$.

Clearly, for a solute in a solvent, the magnitude of this effect is potentially dependent upon the relative strength of interaction between the solute and the solvent versus the solvent–solvent interaction.^{1,2,6–8} In a neat fluid, such distinction is irrelevant, and for this reason LDE effects are less marked. It has been theoretically assessed that LDE phenomena in neat fluids is certainly difficult to assess due to the fact that the vibrational modes are mostly sensitive to interactions with closest neighboring molecules.⁹ However, LDE effects still exist and have been shown evident in a few vibrational spectroscopic studies.^{10–16} Nevertheless, these effects have been detected using Raman scattering on static (band center positions) and dynamic (rotational correlation times) observables leading to consistent results about the trend of LDE enhancement with bulk density.^{15,16}

In that context, CO_2 is quite challenging, as it is certainly the widest used SC fluid in terms of application. The aim of this paper is to investigate this fluid using Raman spectroscopy in order to demonstrate LDE effects. Prior to that study, it is worthwhile mentioning that for this fluid, a complication arises and should be taken into account.

In a previous investigation using Raman spectroscopy, we have shown that in neat SC carbon dioxide, the state of aggregation should be taken into account in a broad density range extending from gas to liquid-like density.¹⁷ More pre-

* To whom correspondence should be addressed. Tel: +351 21 7904877. Fax: +351 217954288. E-mail: Isabel@cii.fc.ul.pt.

[†] Centro de Física Atómica da UL.

[‡] Institut des Sciences Moléculaires, CNRS, Université Bordeaux.

cisely, we found that two types of environments are detected on the finite time scale of observation of the spectroscopic technique. The first one involves “standard” physical forces (Lennard–Jones type) between a tagged CO₂ molecule with the molecules constituting its first shell leading to the so-called “free” CO₂ molecules. The second one is related to the formation of a homo-dimer (the so-called “complex”). This conclusion was reached from the analysis of the ν_2 Raman inactive (for the isolated molecule) bending mode centered at 667 cm⁻¹ and from the study of the two intense {21} and {2u} components of the Fermi doublet, situated at 1285 cm⁻¹ and 1388 cm⁻¹, as well as from the spectral feature put in evidence in the spectral domain between these two peaks. In the context of the present investigation, it is noteworthy that we found that each of the Fermi dyad peaks resulted from the overlap of two components associated with the two particular environments of CO₂ to which we previously referred.

The main issue raised in this paper is to provide evidence about the existence of LDE in carbon dioxide at intermediate and liquid-like density values using spontaneous Raman scattering. For this purpose, we have taken advantage of using supercritical conditions that offer the possibility of continuously tuning the density of the fluid from gas to liquid-like values. The measurements have been performed on the Fermi dyad. The aim was to investigate the shifts and widths of the two lines constituting each of the Fermi dyad peaks of the ¹²C¹⁶O₂ molecule, as well as the satellite band corresponding to the ¹³C¹⁶O₂ molecule (1% isotopic natural abundance), and the influence of the LDE phenomenon, taking into account the fact that different molecular environments (aggregation) exist.

The results obtained will be subsequently compared with those proposed in a recent MD simulation, and the two viewpoints will be discussed with special attention to their interconnection and differences.

2. Experimental Section

The polarized I_{VV} and depolarized I_{HV} Raman spectra were measured on a Jobin Yvon LabRam HR8000 spectrometer using a back scattering geometry and a Spectra Physics laser operating at a wavelength of 752.4 nm with 100 mW power. A 100- μ m slit and a 1800-lines/mm grating ensured we would have a spectral resolution of 0.5 cm⁻¹.

For each thermodynamics point studied, two spectra have been accumulated during time ranging from 200 s at high CO₂ density to 400 s at low density. The wavenumber calibration has been performed before each series of isothermal measurements using the emission lines of a neon bulb. Spectra were collected in the spectral range from 1262 to 1414 cm⁻¹. We have followed the CO₂ Fermi dyad along three supercritical isotherms (307, 309, and 323 K, with an uncertainty of 0.5 K) by changing the pressure between 0.1 and 35 MPa using the high-pressure bench described elsewhere.¹⁸ Anhydrous CO₂ was provided by Air Liquide with purity higher than 99.995%.

In Figure 1, we have reported for each temperature the evolution with the pressure of the density expressed in reduced units ρ^* . Figure 1 clearly shows the nonlinear dependence of density versus pressure which will play a significant role in the interpretation of spectral data.

The depolarization ratio, which has almost the same value for the two components of the dyad, slightly increases with the density with a mean value equal to 0.07 ± 0.01 . Therefore, the polarized profiles that can be identified with the isotropic profiles $I_{\text{iso}} = I_{\text{VV}} - 4/3 I_{\text{HV}}$ will only be presented in the following.

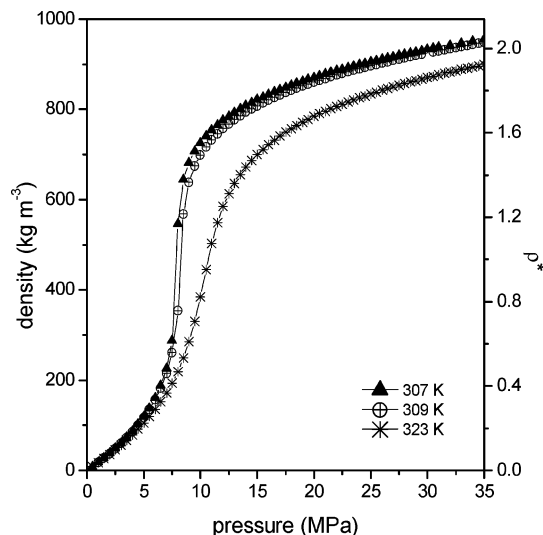


Figure 1. Evolution with pressure of the density of CO₂ at 307 K (▲), 309 K (○) and 323 K (*).

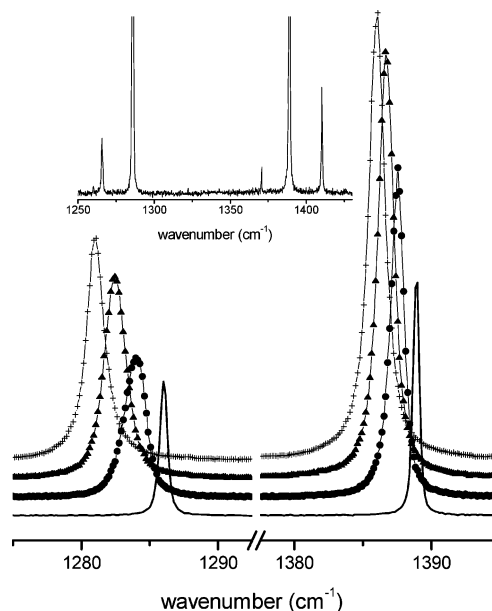


Figure 2. Polarized Raman spectra of CO₂ in the Fermi dyad domain at 307 K: (—) $\rho^* = 0.18$ (top and bottom); (●) $\rho^* = 0.62$; (▲) $\rho^* = 1.17$; (+) $\rho^* = 2.0$ ($\rho^* = \rho/\rho_c$).

3. Results

The Raman active ν_1 totally symmetric stretching vibration of CO₂ (1305.4 cm⁻¹) is in Fermi resonance with the $2\nu_2$ overtone of the bending mode centered at 667 cm⁻¹. As typical examples of the spectral observations in this domain, we have reported in Figure 2 the I_{VV} spectra measured at different pressure values (covering densities from gas-like to liquid-like) at a temperature of 307 K. In this spectral range, we observe the two intense peaks of the Fermi doublet, situated at 1285 cm⁻¹ and 1388 cm⁻¹, respectively, assigned to the {21} and {2u} components according to the notation of Montero.¹⁹ We also note the presence of several very weak satellite bands situated at 1409.5, 1370, and 1265 cm⁻¹ (top of Figure 2). The first one is assigned to the hot band corresponding to the transition $|1\pm\rangle \rightarrow |3u\pm\rangle$, the second one corresponds to the $|0\rangle \rightarrow |2u\rangle$ transition of the ¹³C¹⁶O₂ molecule (1% isotopic natural abundance). The last one, results from the superposition of the hot band assigned to the $|1\pm\rangle \rightarrow |3l\pm\rangle$ transition of the ¹²C¹⁶O₂ molecule with the $|0\rangle \rightarrow |2l\rangle$ transition of the ¹³C¹⁶O₂ molecule.¹⁹

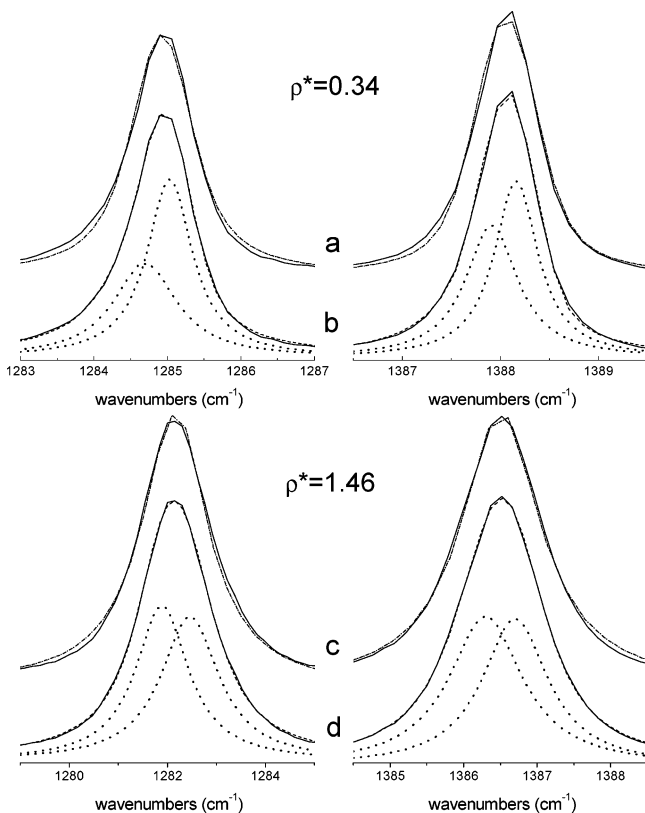


Figure 3. Comparison of experimental polarized Raman spectra of CO₂ in the Fermi dyad domain at 307 K for $\rho^* = 0.34$ (top) and $\rho^* = 1.46$ (bottom) with fitted profiles to each dyad component: (a) and (c) one Lorentzian; (b) and (d) two Lorentzian profiles (see text).

3.1. The {2l} and {2u} Fermi Dyad. The Raman spectra measured along the isotherm 307 K displayed in Figure 2 show that as the density increases, the components of the doublet are shifted toward lower wavenumbers. Concomitantly, they broaden and the intensity of the {2u} component increases relative to the {2l} one. This overall trend is in agreement with previous investigations reported in the literature.²⁰ To get a more quantitative insight, the spectra have been analyzed by fitting each component of the dyad band shapes with a single Lorentzian profile, taking into account the experimental resolution. It turns out that although fair fits are obtained, there still exist some marked discrepancies between the calculated and experimental band shapes. It is only by fitting each doublet component with two Lorentzian profiles convoluted by the experimental resolution that better fits have been achieved (Figure 3). The need for using two Lorentzian profiles for fitting each component of the Fermi dyad is mainly important for density values of ρ^* smaller than 1.7. In fact, it is for liquid-like density values that the difference between fitting one or two profiles is less pronounced.

For the sake of clarity in the following, we will denote the two fitted Lorentzian profiles in the high-frequency component of the Fermi doublet as U₁ and U₂ (U as upper). Label 1 (resp 2) characterizes the fitted profile centered at the lowest frequency (resp higher). This convention will be applied to the lowest component of the Fermi dyad denoted L₁, L₂ (L as lower).

The evolution with density of the parameters corresponding to the frequency positions and the widths (fwhh) of the peaks L₁, L₂ and U₁, U₂ is displayed for the isotherm 307 K in Figures 4 and 5, respectively.

We found that the band-center frequency values of the four fitted Lorentzian profiles decrease with increasing density

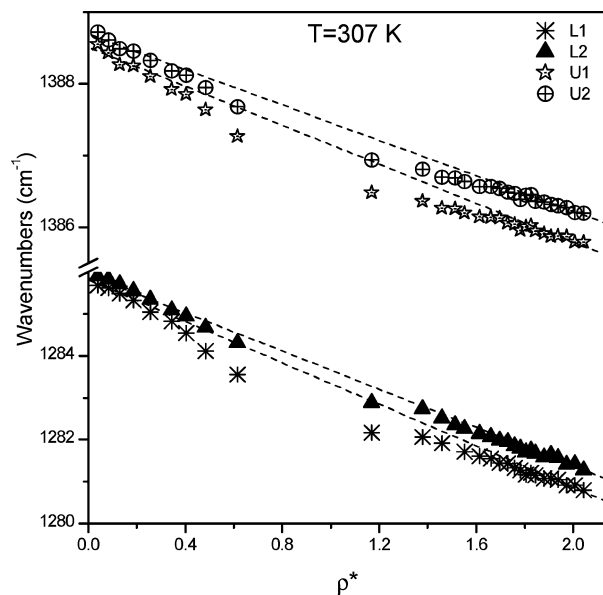


Figure 4. Evolution with the density of the band-center position of fitted profiles to the Fermi dyad peaks at 307 K.

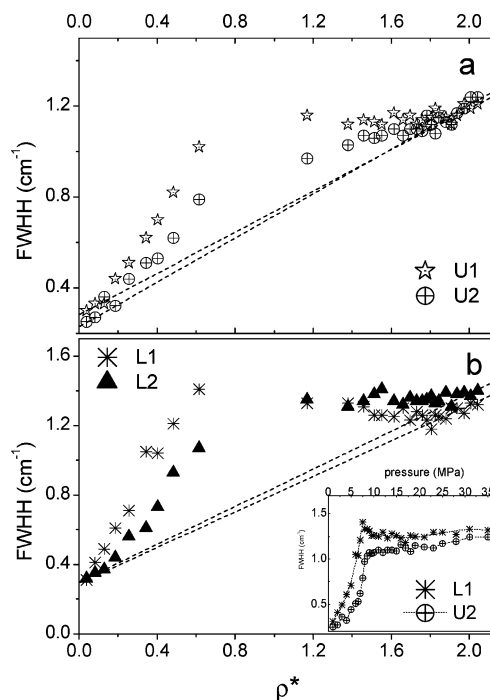


Figure 5. Evolution with the density of the fwhh of fitted profiles to Fermi dyad peaks at 307 K: (a) Upper components, (b) Lower components. The evolution with pressure is shown in inset.

(Figure 4). This observation is consistent with earlier works but must be contrasted with the fact that in previous investigations,²⁰ each of the Fermi doublet components has been considered to be constituted by a single profile. We also noticed that the band centers of the U₁, U₂ and L₁, L₂ profiles are almost co-incident at very low density but depart significantly as the density increases. In addition, we observed that the evolution of the band center with density is nonlinear, as indicated from comparison with a linear function. All of these experimental observations are found to apply for the three isotherms investigated.

The values of the widths of the U₁, U₂ and L₁, L₂ components are found to markedly increase with density (Figure 5). It is noteworthy that a common trend is observed in which the values of the widths steeply increase in the 0.1–0.6 reduced density

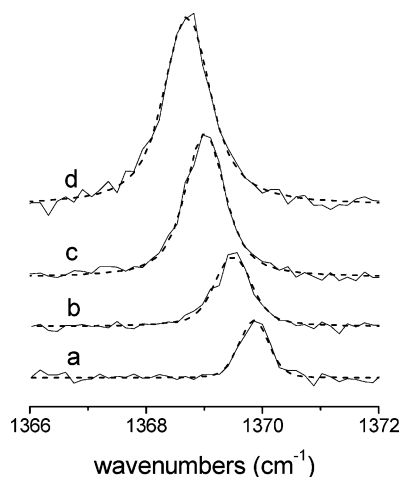


Figure 6. Polarized Raman spectra associated with the $|0\rangle \rightarrow |2u\rangle$ transition of the $^{13}\text{C}^{16}\text{O}_2$ (1% isotopic natural abundance), at 307 K for different reduced density values ρ^* ($\rho^* = \rho/\rho_c$): 0.34 (a); 0.62 (b); 1.17 (c); and 2.01 (d).

range to reach an ill-defined kind of “plateau” for ρ^* in the range from 0.6 to 1.6 and then increase again. The values of the widths of the U_1 , U_2 profiles (as well as the L_1 , L_2 profiles) are very close to each other at very low density, depart from each other at intermediate density (0.4 to 1.0 range) and become again almost equal at the highest density investigated (1.0 to 2.0 range). At this level, it is also interesting to contrast the evolution of the values of the widths using either the density or the pressure. This can be done using the components L_1 and U_2 , as displayed in the inset of Figure 5b. As the pressure increases the widths increase sharply (range 0–6 MPa) to reach an almost constant value in the range from 10 to 35 MPa. We note in particular a kind of “overshoot” at the transition between the two regimes at a pressure ~ 8 MPa for the L_1 component which is not observed for U_2 . This “accident” has been reported, and its origin is discussed for the lower Fermi dyad component treated as a single line.^{12,21} Clearly, it appears smoothed using a density representation. This is due to the fact that the evolution of density with pressure (see Figure 1) is also highly nonlinear, and thus partly compensates the nonlinearity observed in the evolution of the width with pressure.

At the same density, the profiles involved in the lower component of the Fermi dyad are always found to be broader than those associated with the higher frequency component. All of the trends reported so far for the widths have been found to be the same for the three isotherms investigated.

3.2. The $|0\rangle \rightarrow |2u\rangle$ Transition of the $^{13}\text{C}^{16}\text{O}_2$ Molecule. The $|0\rangle \rightarrow |2u\rangle$ transition of the $^{13}\text{C}^{16}\text{O}_2$ (consistent with the isotopic abundance) is extremely weak and barely detectable, and its intensity is only about 2% of the corresponding transition of the $^{12}\text{C}^{16}\text{O}_2$ molecule. Typical profiles recorded along the 307 K isotherm are displayed in Figure 6, which also illustrates the quality of our experimental data. The band shapes have been found to be nicely fitted by a single Lorentzian convoluted by the experimental resolution. The values of the fitted band centers and fwhh are reported as a function of the density in Figure 7, parts a and b. The values of the adjusted widths were always found to be smaller than that of the corresponding spectral transition for the natural abundance molecule. As for the $^{12}\text{-CO}_2$, we found that the values of the band center decrease as the density increases, also exhibiting a nonlinear behavior (Figure 7a). The evolution of the fwhh with the density is also found to be increasing in a nonlinear manner (Figure 7b). However, the nonlinearity observed here is far less dramatic

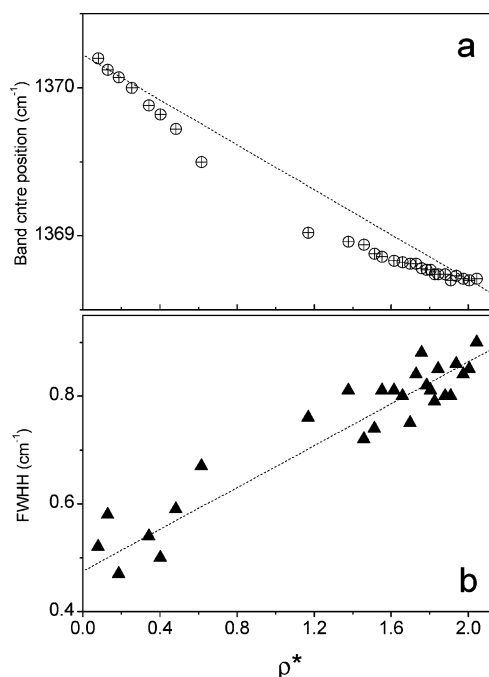


Figure 7. Evolution with the density of the band center position (a) and fwhh (b) of fitted profiles to the $|0\rangle \rightarrow |2u\rangle$ transition of the $^{13}\text{C}^{16}\text{O}_2$ (1% isotopic natural abundance), at 307 K.

than that observed for the corresponding transition in the $^{12}\text{C}^{16}\text{O}_2$ molecule, and the values of the widths are always significantly smaller (roughly by 50%).

4. Discussion

We have relied on the type of analysis which, although only empirically grounded to process experimental data, has been found to be successful when comparing findings with theoretical predictions. For that purpose, we have used the approach that consists of comparing the observed band center evolution with the linear trend expected for a homogeneous fluid. On this basis, we empirically demonstrated that for neat SC fluid, the deviation from this theoretically expected behavior of homogeneous fluid could be interpreted as resulting from local density enhancements encountered in SCF. We also found that this type of analysis could be applied to the evolution of the fwhh, leading to consistent results with band center analysis on the LDE effects. Therefore, we have used this approach to analyze the density evolution of band center and fwhh reported here. In practice, this led us to assume that it is only at very low (gaseous density) or very high (liquid-like density $\rho^* \geq 2$) densities that the band centers (or fwhh) are recovering the values expected for the homogeneous fluid. Then, the empirical method consists in fitting a straight line using the band center values measured in these two density domains and to consider that any departure from this linear evolution can be ascribed to the signature of the LDE phenomenon. The standard approach developed so far to quantify the evolution of the local density, ρ_{loc} , compared to the bulk density, ρ_{bulk} , has been described elsewhere.^{1–3} Let us briefly recall that the local density, ρ_{loc} , can be obtained as follows. The band center, say ν_{meas} , measured at a particular density, ρ_{bulk} , is considered to have the same value as that of a hypothetical homogeneous fluid. Plugging the value ν_{meas} into the equation of the fitted straight line supposed to describe the density evolution of the band center frequency of the hypothetical homogeneous fluid gives the corresponding local density, ρ_{local} . The reduced local density excess is then defined as $\Delta\rho^* = \rho_{\text{loc}}^* - \rho_{\text{bulk}}^* = (\rho_{\text{loc}} - \rho_{\text{bulk}})/\rho_c$.

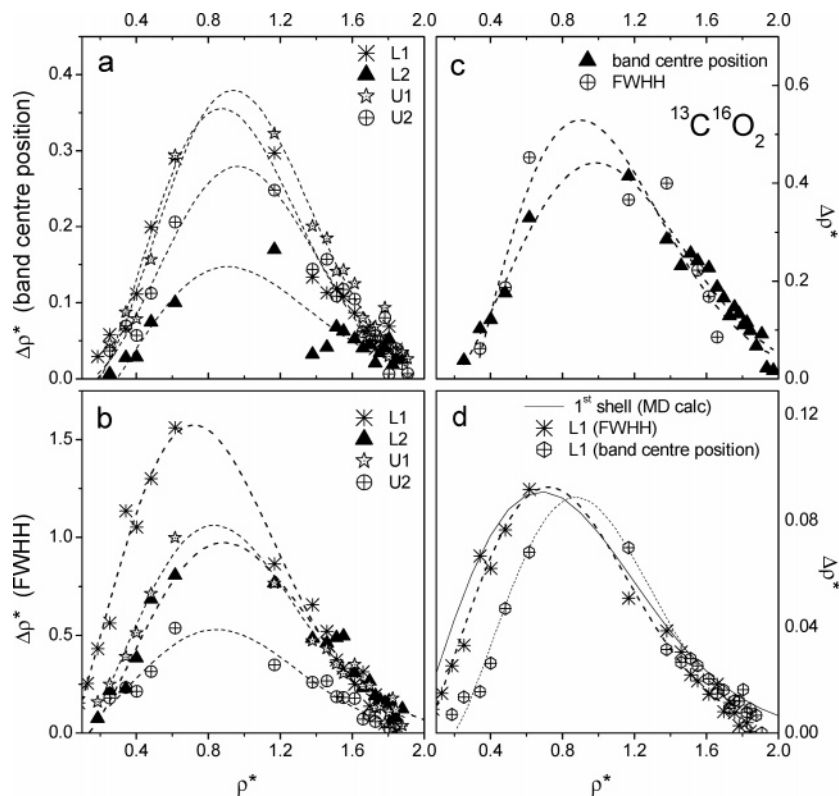


Figure 8. Evolution with the density of reduced local density excess $\Delta\rho^*$ at 307 K calculated from (a) band-center position and (b) fwhh for the upper and lower components of the dyad; (c) band-center position and fwhh of the $|0\rangle \rightarrow |2u\rangle$ transition of the $^{13}\text{C}^{16}\text{O}_2$ molecule (1% isotopic natural abundance); and (d) comparison of $\Delta\rho^*$ obtained from the L_1 component scaled on the calculated distribution of Samios et al.²² (see text).

We have applied this method to the measured band centers and fwhh. The evolution of these two observables with the reduced density ρ^* is displayed in Figure 8, parts a and b, respectively, for the 307 K isotherm. It turns out that LDE effects are clearly evidenced on all of the measured observables corresponding to the U and L components involved in the $\{2l\}$, $\{2u\}$ Fermi dyad. This is seen from the broad and asymmetric distributions presenting an ill-defined maximum in the 0.7–1.0 reduced density range.

Before applying the same treatment to the $|0\rangle \rightarrow |2u\rangle$ transition of the $^{13}\text{C}^{16}\text{O}_2$ molecule, we should recall that a single Lorentzian was only needed to fit the band shape. We surmised that only the transition involving the isolated $^{13}\text{CO}_2$ can be detected as the perturbed transition corresponding to the $^{13}\text{C}^{16}\text{O}_2\text{--CO}_2$ dimer must be too weak to contribute significantly. Nevertheless, LDE effects are clearly detected on the observables associated with the transitions (Figure 8c).

To compare the shape of the LDE evolution with the density, we have used a four parameter Weibull distribution function that was previously proposed to fit the LDE data.^{4,8,22} This distribution is given by the following:

$$\Delta\rho^* = \alpha\chi^{-\chi} \left[\frac{\rho^* - \rho_0^*}{\beta} + \chi^{1/c} \right]^{c-1} \times \exp \left\{ - \left[\frac{\rho^* - \rho_0^*}{\beta} + \chi^{1/c} \right]^c + \chi \right\}, \quad \chi = \frac{c-1}{c} \quad (1)$$

in which α is the amplitude of the maximum of the distribution observed at the density ρ_0^* . This expression has been fitted on the experimental results displayed in Figure 8 and the adjusted parameters are given in Table 1. We observe that the value of the density ρ_0^* corresponding to the maximum of the distribution obtained from the band center position is ranging from 0.88 to

TABLE 1: Fitted Parameters of the Weibull Distribution (eq 1) of the Local Density Excess $\Delta\rho^* = \rho_{\text{loc}}^* - \rho_{\text{bulk}}^* = (\rho_{\text{loc}} - \rho_{\text{bulk}})/\rho_c$ Obtained from the Band Center Position and from fwhh of the Fitted Lorentzian Profiles L_1 , L_2 and U_1 , U_2 to the $\{2u\}$ and $\{2l\}$ Fermi Dyad Components, Respectively^a

observables	transitions	α	β	c	ρ_0^*
band-center position	L_1	0.36	0.88	2.3	0.88
	L_2	0.15	0.85	2.1	0.91
	U_1	0.38	0.94	2.4	0.94
	U_2	0.28	1.0	2.6	0.96
fwhh	L_1	1.6	0.91	2.2	0.72
	L_2	0.97	0.97	2.3	0.89
	U_1	1.1	0.94	2.3	0.83
	U_2	0.53	1.0	2.4	0.85
band-center position	$\{2u\}$ $^{13}\text{C}^{16}\text{O}_2$	0.44	1.0	2.3	0.99
	$\{2u\}$ $^{13}\text{C}^{16}\text{O}_2$	0.53	0.83	2.0	0.90

^a The fitted parameters obtained from $|0\rangle \rightarrow |2u\rangle$ transition of the $^{13}\text{C}^{16}\text{O}_2$ molecule (1% isotopic natural abundance) are also presented.

0.96, whereas the dispersion is greater for ρ_0^* taken from the widths (0.72–0.89).

The first conclusion stemming from these observations is that indeed LDE can be observed on neat fluids, as it was pointed out in the Introduction. It is also important to note that LDE effects are still detected on the two other isotherms investigated. It is expected from theoretical arguments and experimentally verified that LDE effects become vanishingly small as the temperature is increased. This is easily understood on physical grounds, as the fluid is expected to become more and more homogeneous as the temperature is increased and departs from the critical temperature. An indicator widely used is the reduced temperature $T^* = T/T_c$, and it has been shown that when T^* exceeds 1.1 or so, LDE effects should be strongly reduced.^{2,5}

Another issue coming out from the examination of Figure 8a is contained in the fact that at a particular density, the magnitude of the reduced density excess obtained from band center measurements is dependent upon the particular transition used to characterize it (Figure 8a). A glance at Figure 8b shows that this conclusion applies as well for the fwhh. Of course, it is not expected that at a given density and for the same vibrational transition, the magnitude of the reduced excess density obtained from band center and fwhh should be equal. Indeed, these observables probe molecular interactions differently in the fluid. Band center shifts are related to the first and second derivatives of the intermolecular potential calculated for the molecule in its distorted equilibrium geometry, and therefore correspond to a static information. On the contrary, widths are related to relaxation phenomena (mostly vibrational relaxation here) which are in essence dynamical processes.

Nevertheless, we have compared the shape of the LDE evolution with the density obtained from band centers position and widths after scaling the corresponding distribution to the same maximum value. The result is displayed in Figure 8d and illustrated for the L₁ component of the {21} transition of the Fermi dyad for which the experimental dispersion is the highest. It turns out that it is mainly the magnitude and not the shape of the distribution itself which is dependent upon the particular observable used to put in evidence LDE. It is noteworthy that the present results confirm the conclusions that we reached in our previous Raman investigation on neat SC hexafluorobenzene.^{13,15,16} Finally, it turns out that even empirical, the approach used here, is rather heuristic. At this level, we can compare our findings with those obtained recently by Samios et al. using MD simulations.²² For that purpose, we have reported in Figure 8d the distribution calculated by these authors for the first shell of molecules surrounding a tagged CO₂ molecule for the fluid at 313 K after scaling to these results, obtained from the L₁ component. The nice result coming out from this comparison is that the calculated and experimental distributions are very close to each others, in particular for that associated with fwhh and display the same broad and asymmetric shape. However, we note that the predicted density maximum is observed at slightly lower reduced density (0.68). Considering also the second shell does not change the observed trend. We may invoke that the experiments have been performed at a temperature closer to the critical point than that in the MD calculation. Nevertheless, the agreement obtained here is rather impressive considering the fact that experimentally, the LDE has been extracted using the empirical method discussed previously on different observables, whereas it was directly obtained from coordination numbers in the MD calculation.

5. Conclusion

We come to the final conclusion that in neat SC carbon dioxide, not only does LDE exist and affect the shifts and fwhh of spectral transition of the molecules but also that dimers exist and that their spectral transition are affected as well by this phenomenon.

This picture is different and complementary from that provided by MD simulation. Simulations put emphasis on processes involving two neighboring shells of molecules around a tagged molecule. In contrast, we are discussing interactions within the first shell. More precisely, we are putting the emphasis between the existence of two types of environments for a tagged molecule in its first shell. The first one involves the interaction of the tagged molecule itself with the molecules constituting the shell, whereas the second one concerns a

“specific” interaction leading to the formation of a dimer (the so-called “complex”).

From this viewpoint, this physical description is strongly connected to the theories proposed to treat Raman spectra of reactive fluids in which chemical exchange exist. We believe that the proposed description corresponds to a dynamical situation that is close to the so-called “slow exchange regime” for which different environments of the probe molecule can be detected on the finite time scale of observation. In that context, no theoretical approaches have been proposed to treat fast chemical reactions from the Raman spectra of vibrations experiencing the Fermi resonance phenomenon. Clearly, the pictures proposed here and in the MD simulation are not mutually exclusive and certainly somehow interrelate as such decomposition of the effect of interactions in the fluid are hard to disentangle. These results show the richness of the spectra of such “simple fluids” as investigated in the supercritical domain and reveal that more exciting work should remain to be performed to certainly propose an overall consistent understanding of the interactions in SC carbon dioxide.

Acknowledgment. The authors thank the Université Bordeaux I for the attribution of an ATER position for S.L. and the financial support of the joint CNRS–INICT PICS Program No. 3090, which provided travels and stays facilities for two of the authors (M.I.C. and M.B.) to complete part of this work is gratefully acknowledged. It is also a pleasure to thank our colleagues D. Talaga and Dr T. Tassaing for valuable help in Raman experiments and for guidance in using the high-pressure set up.

References and Notes

- (1) Kajimoto, O. *Chem. Rev.* **1999**, *99*, 355.
- (2) Tucker, S. C. *Chem. Rev.* **1999**, *99*, 391.
- (3) Song, W.; Biswas, R.; Maroncelli, M. *J. Phys. Chem. A* **2000**, *104*, 6924.
- (4) Lewis, J. E.; Biswas, R.; Robinson, A. G.; Maroncelli, M. *J. Phys. Chem. B* **2001**, *105*, 3306.
- (5) Song, W.; Maroncelli, M. *Chem. Phys. Lett.* **2003**, *378*, 410.
- (6) Debenedetti, P. G.; Mohamed, R. S. *J. Chem. Phys.* **1989**, *90*, 4528.
- (7) Maroncelli, M. *J. Phys. Chem. A* **2000**, *104*, 6924.
- (8) Nugent, S.; Ladanyi, B. M. *J. Chem. Phys.* **2004**, *120*, 874.
- (9) Egorov, S. A.; Skinner, J. L. *J. Phys. Chem. A* **2000**, *104*, 483.
- (10) Echargui, M.; Marsault-Herail, F. *Molec. Phys.* **1987**, *60*, 605.
- (11) Ben-Amotz, D.; LaPlant, F.; Shea, D.; Gardecki, J.; List, D. *Supercritical Fluids Technology*. In *ACS Symposium Series*; Bright, F., McNally, M. E., Eds.; American Chemical Society: Washington DC, 1992; Vol. 488; p 18.
- (12) Nakayama, H.; Saitow, K.; Nakashita, M.; Ishii, J.; Nishikawa, K. *Chem. Phys. Lett.* **2000**, *320*, 323.
- (13) Cabaço, M. I.; Besnard, M.; Danten, Y.; Tassaing, T. “Local density inhomogeneities in the supercritical domain studied by Raman scattering”; 8th Meeting on Supercritical Fluids, ISASF 2002, Bordeaux.
- (14) Saitow, K.; Otake, K.; Nakayama, H.; Ishii, K.; Nishikawa, K. *Chem. Phys. Lett.* **2003**, *368*, 209.
- (15) Cabaço, M. I.; Besnard, M.; Tassaing, T.; Danten, Y. *J. Mol. Liq.* **2006**, *125*, 100.
- (16) Cabaço, M. I.; Tassaing, T.; Danten, Y.; Besnard, M. *Pure Appl. Chem.* **2004**, *76*, 141.
- (17) Cabaço, M. I.; Longelin, S.; Danten, Y.; Besnard, M. **2007**, submitted.
- (18) Lalanne, P.; Rey, S.; Cansell, F.; Tassaing, T.; Besnard, M. *J. Supercrit. Fluids* **2001**, *19*, 199.
- (19) Montero, S. *J. Chem. Phys.* **1983**, *79*, 4091.
- (20) Garrabos, Y.; Echargui, M. A.; Marsault-Herail, F. *J. Chem. Phys.* **1989**, *91*, 5869, and references therein.
- (21) Arakcheev, V. G.; Bagratashvili, V. N.; Valeev, A. A.; Gordiyenko, V. M.; Kireev, V. V.; Morozov, V. B.; Olenin, A. N.; Popov, V. K.; Tunkin, V. G.; Yakovlev, D. V. *J. Raman Spectrosc.* **2003**, *34*, 952.
- (22) Skarmoutsos, I.; Samios, J. *J. Chem. Phys.* **2007**, *126*, 44503.